Calculation of Transport Coefficients of Air Plasmas

J. Bacri[1] and S. Raffanel[1]

This paper is devoted to results of calculation of the main transport coefficients of air plasmas: electrical and thermal conductivities and viscosity. These calculations are performed for pressures between 1 and 200 atm and for temperatures varying from 1000 to 30,000 K. The computational methods proposed by Devoto from the classical formalism described by Hirchfelder et al. are used. Collision integrals for interactions between charged particles are calculated using the formalism of Mason et al. to account for the fact that, in most of the situations considered here, the number of charged particles in the Debye sphere is weak.

1. INTRODUCTION

When a system (gas or liquid) is subjected to internal or external constraints such as concentration, velocity or temperature gradients, or electric field, as a reaction, one or several of the following nonequilibrium terms then develops: diffusion current, pressure, heat flux, or electric current. When the constraint is weak enough to induce only a small perturbation on the velocity distribution function, a proportionality between the cause and the effect exists and the factor of proportionality is the so-called transport coefficient.

These transport coefficients are depending both on the population number densities of the different species of the system and on the nature and frequency of collisions between these particles.

In the preceding paper,[1] results concerning composition and thermodynamic functions of air plasmas in extended ranges of pressure and temperatures were presented. In this paper, we present results concerning the calculation of the main transport coefficients, i.e., thermal and electrical conductivities and viscosity. These three parameters are particularly needed

[1] Centre de Physique Atomique, Unité Associée au CNRS No. 277, Université Paul Sabatier, 118 route de Narbonne, 31062 Toulouse Cedex, France.

to solve energy rate equations such as the Ellenbaas–Heller equation or to model plasma flows produced in high-power torches. The numerical results of these calculations have been published as an internal report[2] available from the authors.

2. SUMMARY OF FUNDAMENTALS OF TRANSPORT COEFFICIENT CALCULATIONS

In this work, the basis of calculation of the transport coefficients is the resolution of the Boltzmann collision equation by a first-order perturbation technique proposed by Chapman and Enskog.[3,4] Chapman and Cowling[3] have shown that the transport coefficients can be expressed in terms of Sonine polynomial expansion coefficients. These coefficients are combinations of a set of integrals which contain information on the dynamics of the collisions between the components of the system. These so-called collision integrals are defined for interactions between molecules i and molecules j by

$$\Omega_{ij}^{(l,s)} = \frac{2\pi kT}{\mu_{ij}} \int_0^\infty \int_0^\infty \exp\left(-\gamma_{ij}\right) \cdot \gamma^g 2^{s+3} (1-\cos^l \chi) b \, db \, d\gamma_{ij} \qquad (1)$$

where γ_{ij} is the reduced initial relative speed of the colliding molecules, χ their angle of deflection measured in the center-of-gravity coordinate system, and b the impace parameter. The term μ_{ij} is the reduced mass of the two interacting particles. The interaction potential between the components of the system appears clearly through the correlations between b, x, and γ_{ij}.

The classical transport cross section denoted $Q^{(1)}$ is defined as

$$Q^{(1)} = 2\pi \int_0^\infty (1-\cos^l \chi) b \, db \qquad (2)$$

The transport coefficients are often expressed in terms of collision integrals $\bar{\Omega}_{ij}^{l,s}$ defined by

$$\bar{\Omega}_{ij}^{(l,s)} = (r_i + r_j)^2 \Omega_{ij}^{*(l,s)} \qquad (3)$$

where r_i and r_j are the radii of particles i and j and

$$\Omega_{ij}^{*(l,s)} = \Omega_{ij}^{(l,s)} / \Omega_{ij}^{(l,s)} \text{R.S.} \qquad (4)$$

$\Omega_{ij}^{(l,s)}$R.S. is the value of the collision integral calculated assuming that the interaction potential being i and j is the rigid-spheres potential i.e., $V(r) = 0$ if $r > (r_i + r_j)$; $V(r) = \infty$ if $r < r_i + r_j$; r_i and r_j are the radii of the colliding particles.

Under the pressure and temperature conditions considered in these calculations, the population number densities of charged particles are particularly high: the electron population number density exceeds 10^{19} cm^3 for

$p = 100$ atm when $T > 20,000$ K. Due to the long range of the interaction potential between these particles, the corresponding collision integrals should be treated with special attention.

3. COLLISION INTEGRALS FOR CHARGED PARTICLE–CHARGED PARTICLE INTERACTIONS

Because the classical Coulomb potential falls off too slowly with the distance, interactions between charged particles should be described by a shielded Coulomb potential (S.C.P.) of the form

$$V(r) \sim (1/r) \exp(-r/h)$$

where h is the Debye shielding distance.

For transport coefficient calculation, the S.C.P. was first used by Liboff.[5] In this model, a characteristic length of the plasma L was introduced such that $b_0 < L < h$, b_0 being the mean value of the impact parameter for collisions between particles i and particles j $(b_0 = Z_i Z_j e^2 / 2kT)$ and h the Debye length calculated taking into account both electrons and ions. The collision integrals were then calculated using a classical Coulomb potential for impact parameter values smaller than L, and using the S.C.P. when values of b greater than L were considered. The collision integrals are then expressed by the general relations

$$\Omega_{ij}^{(1,s)} = \frac{4b_0^2}{s(s+1)} \left| Ln(2h/b_0) + \psi(s) - 1.654 \right| \tag{5}$$

where $\psi(s) = \sum_1^n 1/n$ with $\psi(1) = 0$,

$$\Omega^{(2,s)} = 3\Omega^{(1,s)} - 6b_0^2/s(s+1) \tag{6}$$

This hypothesis implies that the number of charged particles in the Debye sphere is high enough to obtain the shielding effect.

From the calculation of air plasma compositions discussed in Ref. 1, the number of charged particles in the Debye sphere is obtained. In Fig. 1 the variations of this number as a function of temperature, for different pressures, are shown. Taking these results into account, it may be readily seen that, following the pressure and temperature values, because the two first terms in the brackets of Eq. (5) do not always counterbalance the negative constant, the collision integrals can take negative values, which is a physical nonsense. For instance, for a temperature value of 25,000 K, all collision integrals corresponding to interactions (X^+/Y^{+++}) or (X^{++}/Y^{++}) become negative when pressure exceeds 50 atm.

It should be noted that the collision integrals calculated by Kihara[6] on the same S.C.P. basis also have negative values in more extended temperature and pressure ranges than those in Liboff's theory.
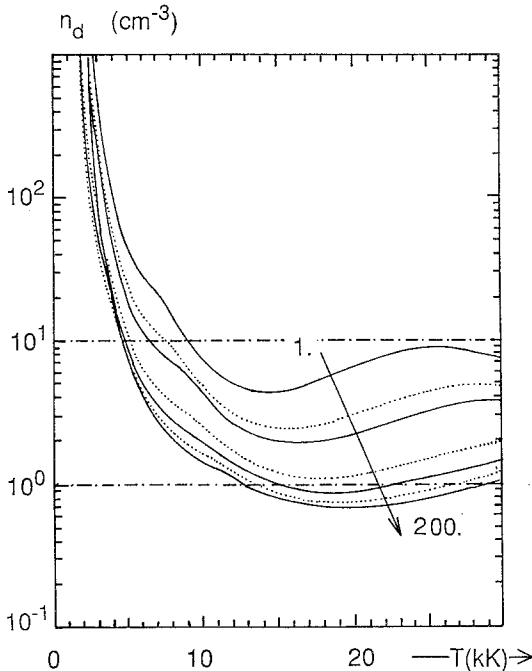
n_d (cm^{-3})

Fig. 1. Number of charged particles in the Debye sphere. The arrow shows the evolution of curves as pressure increases.

Spitzer and co-workers have calculated the collision integrals for charged particle–charged particle interaction in a fully ionized gas from the Fokker-Plank equation.[7,8] They also obtain an analytical form in which the term $Ln(2h/b_0)$ plays a role and which leads to the same difficulties when the number of charged particles in the Debye sphere becomes small.

The model used in this work was proposed by Mason, Munn, and Smith.[9–12] In this model, a S.C.P. was also considered but using a Debye length calculated only from the electron number density. For the calculation of the classical transport cross sections $Q(l)$, the range of integration was broken into three intervals:

—the first corresponds to the smallest values of b $(b < 10^{-3}\,h)$; in this interval, a classical Coulomb potential can be used.

—the second corresponds to intermediate values of the impact parameter, and a distinction between attractive and repulsive potentials should be made.

—for the highest values of b, only interactions leading to small values of the deflection angle χ $(\chi < 0.05\,\text{rad})$ are taken into account. In this

interval, attractive or repulsive potentials give the same result for collision cross sections and consequently for collision integrals. Under these conditions, their asymptotic forms are in agreement with the results of Liboff[5] or Kihara.[6]

As mentioned above, the screening effect exists only when the number of charged particles, n_d, in the Debye sphere is important (100 is the order of magnitude). When this condition is fulfilled, the main term in the collision integrals is the logarithmic term which is $\gg 1$. When strongly correlated plasmas are considered, n_d can be <1 and collisional theories as those proposed by Liboff or Mason and co-workers are not yet valid.

Some of the authors mentioned in Ref. 13 have proposed a "unified" theory which, in principle, allows the extension of these calculations to situations characterized by $n_d \sim 1$ or $Ln(\Lambda) \neq 3$. Nevertheless, for n_d values <1, this "unified" theory diverges when theories using the S.C.P., though nonvalid, do not diverge. This phenomenon is described by Glasser[14] and illustrated by Devoto[15] for partially ionized argon plasma at 1 atm.

If we consider that $n_d = 10$ is a lower limit for the validity of the concept of S.C.P., the collisional theories are only valid for the smallest temperature values: in air, with $p = 1$ atm, $T_{lim} \sim 10,000$ K and for $p = 200$ atm, $T_{lim} \sim 5000$ K.

4. COLLISION INTEGRALS FOR NEUTRAL–NEUTRAL OR NEUTRAL–CHARGED PARTICLE INTERACTIONS

4.1. Neutral–Neutral Interactions

To compute classical transport cross sections and corresponding collision integrals corresponding to interactions between neutral species, three models are used.

a. The rigid-sphere model is used when data necessary for more sophisticated models are unavailable. In this model, collision integrals $\bar{\Omega}_{ij}^{(l,s)}$ are equal to the geometric cross sections and do not depend on temperature. When this model is used, numerical values of radius of atoms or molecules are taken mainly from Ref. 16.

b. The reduced temperature model; when nonpolar molecules are considered, the Lennard-Jones (12–6) potential is used, which reads

$$V(r) = 4\varepsilon \left| \left(\frac{\sigma}{r}\right)^{12} - \left(\frac{\sigma}{e}\right)^{6} \right| \tag{7}$$

The constants ε and σ are characteristic of the interacting particles: ε is the depth of the potential well, and σ is the collision diameter, i.e., the value of r leading to $V(r = \sigma) = 0$.

For nonpolar molecules, a Stockmayer potential (i.e., a Lennard-Jones potential with a third term corresponding to the polarizability of atoms or molecules involved in the collision varying as $1/r^3$) is used. The reduced temperature T^* is then defined by

$$T^* = Tk/\varepsilon \qquad (8)$$

where ε is estimated from the relation

$$k/\varepsilon \sim 0.87/T_b \qquad (9)$$

In this relation, the Boltzmann constant k is expressed in erg/Kelvin. The quantity T_b is the boiling point of the chemical species when two identical particles interact; when the projectile and the target are different, ε_{ab} is then defined by $(\varepsilon_a\varepsilon_b)^{1/2}$ (cf. Ref. 4, p. 168).

In Chapter 8 of Ref. 4, the evolution of Ω^* vs. reduced temperature T^* is shown, and numerical values are given. Using this model, we summarize the numerical values of ε/k in Table 1.

It should be noted that this model cannot always be used particularly when one of the interacting particles is N or O, since liquid-phase atomic oxygen or nitrogen do not exist.

c. When two monatomic species are interacting, the collisions can be described on the basis of the Morse potential used to describe the diatomic molecule formed by these two particles. Collision integrals are then obtained by interpolation of the numerical values in the Tables of Samoilov and Tsitelauri[17,18] or in the tables of Smith and Munn.[19] In the latter, values of Ω^* are generally greater than in Ref. 17 due to the influence of the smallest internuclear distances. When this method is used, the spectroscopic constants needed to compute the dimensionless quantities $\beta = \omega_e/2$ $(B_eD_e)^{1/2}$ and $T^* = kT/D_e$ are taken from the tables of Rosen.[20] This method can also be used to treat interactions between a neutral and heavy-charged particle which can form a charged molecular species like NO^+.

Some collision integrals used in this work have been taken from the literature. For example, numerical values for N_2-N_2, N-N, and N-N_2 interactions are obtained by fitting numerical values obtained by Capitelli and Devoto[21] who consider a Morse potential; this procedure has been used by Eymard[22] to compute properties of equilibrium and nonequilibrium pure nitrogen plasma. In the same way, collision integrals for O_2-O_2,

Table I. Values of ε/k Used in This Work for Identical Colliding Particles

	N_2	O_2	NO	N_2O	NO_2	Ar
ε/k	90.06	103.67	139.48	212.24	338.33	100.52

Table II. Models Used to Treat Neutral–Neutral Interaction[a]

	N$_2$	N	O$_2$	O	NO	N$_2$O	NO$_2$	Ar
N$_2$	21	21	T*	R.S.	T*	T*	T*	T*
N		21	R.S.	R.S./Mo	R.S.	R.S.	R.S.	R.S.
O$_2$			25	25	T*	T*	T*	25
O				25	R.S.	R.S.	R.S.	25
NO					T*	T*	T*	T*
N$_2$O						T*	T*	T*
NO$_2$							T*	T*
Ar								25

[a] Numbers refer to references. R.S.: rigid sphere model; T*: Lennard-Jones potential; Mo: Morse potential (numerical values from Ref. 17).

O–O, O$_2$–O, Ar–Ar, Ar–O$_2$, and Ar–O are taken from the compilation published in Refs. 23–25.

   The different models used to compute neutral–neutral collision integrals are summarized in Table II. In Fig. 2, their numerical values are shown for a temperature of 10,000 K: all the neutral–neutral collision integrals are characterized by the same order of magnitude: some Å^2. When they are calculated from the rigid-sphere model, the collision integrals corresponding to N–O interactions differ from the others by a factor of about 3. Because
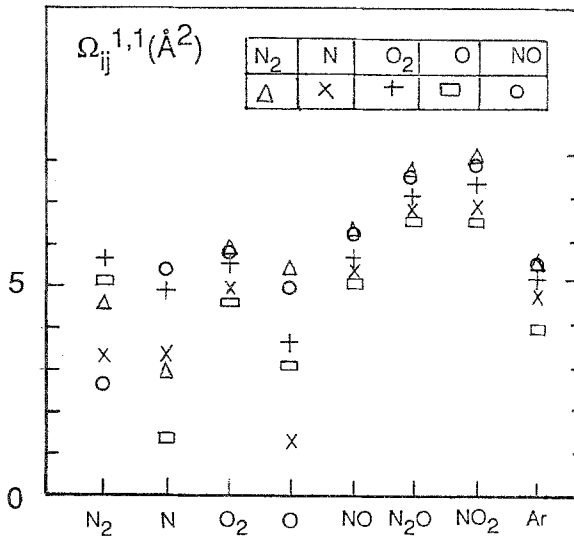

Fig. 2. Comparison of some collision integral values for $T = 10,000$ K calculated by the rigid-sphere model. On the abscissa: target particle; in the table: projectile particle.

N and O are species which play a role in large intervals of pressure and temperature, the influence of these particular collision integrals will be discussed separately.

It should be mentioned that, except for interactions described by the rigid-sphere model which, in principle, lead to constant values, the collision integrals corresponding to interactions between neutral particles vary with temperature more slowly than those corresponding to charged–charged interactions: for example, when the temperature increases from 5000 to 15,000 K the collision integral $\bar{\Omega}^{1,1}$ corresponding to N–N interactions calculated from a Morse potential varies from 4.32 to 2.92 Å^2. The variations with temperature of collision integrals calculated from Lennard-Jones potentials are quite similar.

4.2. Neutral–Charged Heavy Particle Interactions

These interactions have been considered as elastic, and the corresponding collision integrals have been calculated:

—using a Morse potential when possible;

—considering the charge exchange process, mainly when resonant charge exchange occurs, i.e., for reaction such as $X, X^+ / X^+, X$;

—from the polarizability of the neutral atoms or molecules involved in the collisions.

When the polarizability model is used, the collision integrals are then expressed as

$$\Omega_{ij}^{l,s} = \frac{e^2 \xi_i \pi}{\mu_{ij}} \Gamma(s + \tfrac{3}{2}) A_4^l \tag{10}$$

Values of A_4^l are taken from Ref. 26; numerical values of the polarizability ξ_i are either calculated or taken from Ref. 4 or 16. These values are summarized in Table III.

When charge exchange is considered, two situations should be considered:

(a) the resonant charge exchange when the neutral and the charged particle belong to the same chemical species,

Table III. Numerical Values of the Polarizability

Species	N_2	N	O_2	O	NO	N_2O	NO_2	Ar
ξ_i	1.76	1.13	1.60	0.15	1.74	3.00	5.00	1.654
Source	Calc.	4	Calc.	16	Calc.	4	Calc.	16

(b) the nonresonant charge exchange when the two interacting particles belong to different chemical species $(X, Y^+/X^+, Y)$.

Little data on nonresonant charge exchange cross sections are available; these interactions are therefore treated using the polarizability model which, according to the synthesis published by Capitelli[46] leads to an overestimation of collision integrals.

If χ denotes the deviation of the charged particle in a neutral-charged collision, the charge exchange process corresponds to a deviation $(\pi - \chi)$. If P_{ex} is the charge exchange probability, the classical transport cross section is then given by[27]

$$Q^{(l)} = 2\pi \left[\int_0^\infty (1 - P_{ex})(1 - \cos^l \chi) \sin \chi \, d\chi \right.$$

$$\left. + \int_0^\infty P_{ex}(1 - \cos^l (\pi - \chi)) \sin \chi \, d\chi \right]$$

When l is odd, it is obvious that terms depending on P_{ex} disappear; collisions are then wholly elastic. When l is even, then charge exchange plays a role and

$$Q(l) = 2Q^{tr}$$

where, according to Dalgano,[28]

$$Q^{tr} = \tfrac{1}{2}|A - B \log g_{ij}|^2$$

g_{ij} is the relative speed of the interacting particles: A and B are characteristic of the considered species. From their values, the collision integrals can be written as follows:

$$\bar{\Omega}^{l,s} = \frac{1}{\pi} \left\{ A^2 - AB \log (4R) + \left(\frac{B \ln (4R)}{2} \right)^2 + \frac{BX}{2} (B \log (4R) - 2A) \right.$$

$$+ \frac{B^2}{4} \left(\frac{\pi^2}{6} - \sum_{n=1}^{s+1} \frac{1}{n^2} + X^2 \right) + \frac{B}{2} [B (\ln (4R) + X) - 2A] \log \frac{T}{M}$$

$$\left. + \left(\frac{B}{2} \log \left(\frac{T}{M} \right) \right)^2 \right\}$$

R is the perfect gas constant; X is defined from $\sum_{n=1}^{s+1} (1/n - \gamma)$, γ being the Euler constant (0.5772), and M is the molar weight of the considered gas. Numerical values for A and B can be found in several compilations such as that by Rapp and Francis.[29] When A and B are not experimentally known, their values can be calculated from the potential energy curves.[27]

The resonant charge exchange process gives rise to particularly impor-
tant cross sections: in the case of N_2–N_2^+ collisions, for instance, the collision
integral (1,1) corresponding to elastic processes is one order of magnitude
smaller than that obtained from the experimental charge-exchange cross-
section values obtained by Kobayashi for energies smaller than 3 eV[30] and
by Utterback and Miller for energies between 10 and 1000 eV.[31]

In Ref. 21, Capitelli and Devoto indicate that interactions involving
N_2^+ or collisions between N and N^{++} or N^{+++} play a negligible role for
transport-coefficient calculations. For this reason, the collision integrals
corresponding to these processes are given the same values as those for
(NN^+) interactions.

4.3. Neutral–Electron Interactions

Except for the collision integrals corresponding to $NO - e$, $N_2O - e$,
and $NO_2 - e$ interactions, which have been calculated using the above-
mentioned polarizability model, all the collision integrals are taken from
the literature. For $N_2 - e$ interactions, we use collision integrals computed
by Capitelli and Devoto[21] and Penski[32] from experimental cross-section
values in Ref. 33. For $N - e$ interactions, we use the values obtained by
Penski.[32] The collision integrals in which O, O_2, or Ar are involved are
taken from Ref. 25.

5. THE APPROXIMATIONS USED FOR TRANSPORT COEFFICIENT CALCULATIONS

5.1. Thermal Conductivity

The thermal conductivity of a plasma is the ratio between the heat flux
and the corresponding temperature gradient. It can be broken down into
three terms:

—The first term is the translational thermal conductivity related to the
modification of the kinetic energies of the plasma components due to the
temperature gradient. In this term, two contributions can be distinguished:
the contribution of the electrons λ_{tr-e}, and that of heavy particles λ_{tr-h}.
These two terms are calculated using the formalism proposed by Devoto.[34]
Taking into account the convergence between the different approximations
obtained by this author for an argon plasma,[35] we use the third approxima-
tion to calculate the electronic contribution, and the second approximation
to obtain λ_{tr-h}.

—The second term, λ_{int}, is related to the modifications in the distribu-
tion of the excited levels pertaining to the different chemical species and

consequently to the variations of the internal energy of the plasma, induced by the temperature gradient. This term is calculated according to the method developed by Yun et al.[36] from Eucken's theory.

—The third term, λ_{reac}, accounts for the shift of chemical equilibria (ionization, dissociation) due to the temperature gradient. This term is calculated according to the theory of Butler and Brokaw[30,31] adapted to partially ionized gases. In this term, the logarithmic derivatives with respect to temperature of the internal partition function of the species involved in the reaction are needed. This justifies the great care taken to compute these quantities in order to avoid discontinuities during numerical treatments.[1]

5.2. Electrical Conductivity

The electrical conductivity is calculated using the third approximation proposed by Devoto[34] to compute the diffusion coefficients and neglecting the contribution of the ions to the current.

5.3. Viscosity

The static viscosity is calculated using the first-order approximation proposed by Hirchfelder et al. (cf. Ref. 4, pp. 489–490).

6. RESULTS

The calculations were performed for pressure values of 1, 5, 10, 50, 100, 150 and 200 atm. General results concerning the variations of total thermal conductivity, electrical conductivity, and viscosity vs. temperature for the different pressures are shown in Figs. 3–5. These curves have been obtained under the following conditions:

—for N–O interactions, the rigid-sphere model is used.

—for N–N$^+$ interactions, the collision integrals are obtained by fitting the values of Capitelli and Devoto.[21]

—for O–O$^+$ interactions, values obtained by Mexmain[23] and used by Aubreton[24,25] were introduced.

—N$^+$–O and N–O$^+$ interactions are treated by the polarizability model.

In Fig. 6, the variation with temperature of the components of the thermal conductivity obtained for a pressure of 1 atm is shown. It should be mentioned that, except for the higher temperature values ($T > 10,000$ K), and contrary to results obtained for monatomic gases such as argon, the internal thermal conductivity is not negligible: near 2000 K, this component represents about 50% of the total thermal conductivity. This result is mainly
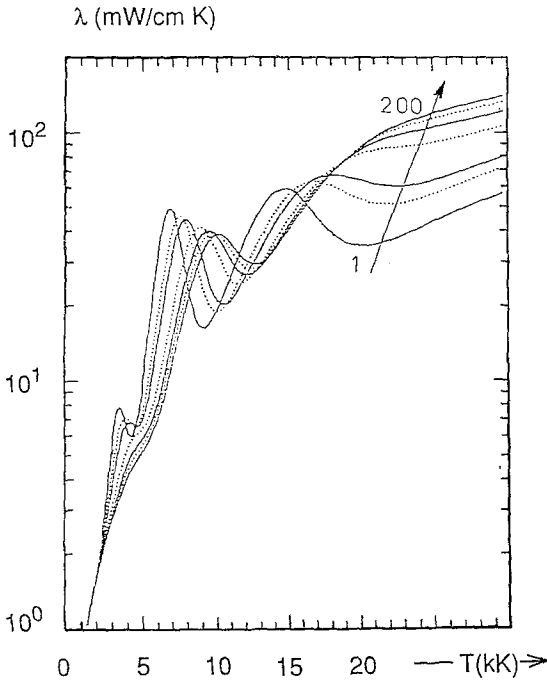
λ (mW/cm K)

Fig. 3. Variation of the thermal conductivity vs. temperature for different pressures.

connected with the chemical composition of the plasma: for the lower temperature values, polyatomic molecules are the most important components. Their internal partition functions are strongly increasing functions of the temperature and give rise to an important contribution to the total thermal conductivity via the internal conductivity.

In Fig. 7, our results are compared with the experimental values obtained by Asinovski *et al.*,[39] by Devoto *et al.*,[47] or with similarly calculated values.[33-35]

Concerning the electrical conductivity, our results are very close to the values obtained by Nicolet *et al.*[42] for temperatures higher than 6000 K. These values are within $15 \sim 20\%$ of the theoretical[40,41] or experimental[39,44] values. For the lowest temperatures characterized by a nonnegligible electrical conductivity ($\sigma > 10^{-3}$ mho/cm), the influence of negative ions (mainly O^-), which are accounted for in our plasma compositions, is to diminish this transport parameter value: these ions constitute a nonnegligible part of the negative charges ensuring the macroscopic electrical neutrality; due to their mass and their geometrical size, their mobility is smaller than that of electrons. Figure 8 is relative to a pressure of 1 atm.
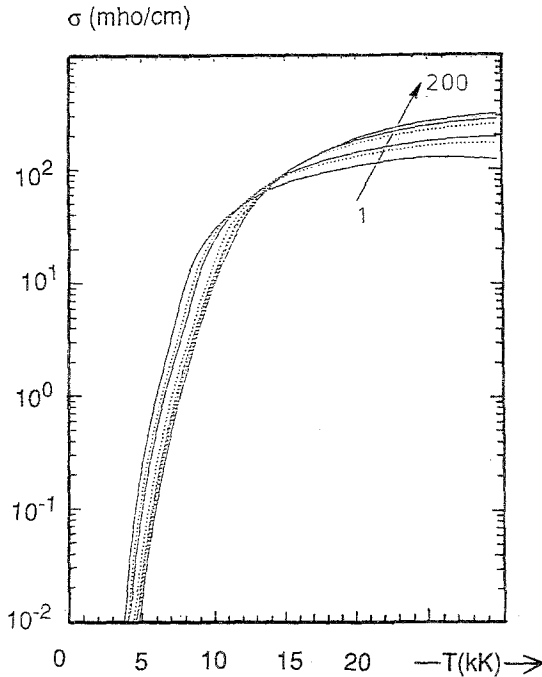
σ (mho/cm)

Fig. 4. Variation of the electrical conductivity vs. temperature for different pressures.

In Fig. 9, different results concerning the viscosity of an air plasma at 1 atm are compared. We obtain satisfactory agreement with the results of Nicolet *et al.*[42] in the whole range of temperatures; up to 15,000 K, maximum values of departure from other works are acceptable. When the temperature reaches or is greater than 20,000 K, discrepancies from the results of Yos[40] arise: a factor of 4 difference between these values and those obtained in our work or in Ref. 42 sometimes appears. Such departures are essentially connected with the plasma composition and with the method used to treat the collision integrals between charges particles:

—as shown in Ref. 42, for a given temperature, when the twofold charged ions N^{++} and O^{++} are neglected, the values of viscosity are increased.

—In addition, in Ref. 40 the collision integrals are not rationally treated: they are computed according to Liboff's model,[5] using an unscreened Coulomb potential up to impact parameter values equal to a Debye length calculated considering only the electron population number density; these collision integrals so obtained are then multiplied by factors ranging from 0.3 to 12 independent of pressure or temperature. These multiplicative
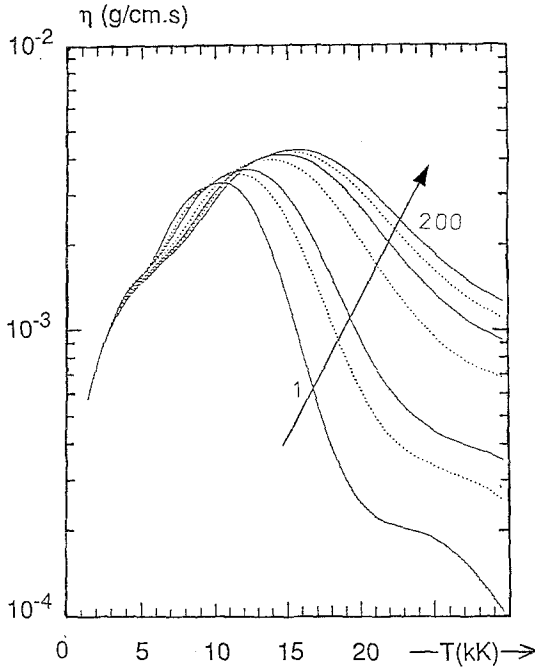
Fig. 5. Variation of the static viscosity vs. temperature for different pressures.

factors are obtained through comparison with electrical and thermal conductivities predicted by Spitzer and Harm[8] for fully ionized gases.

When the pressure value increases, the ionization degree decreases; the concentration of multicharged ions, and by consequence their influence on transport parameters, diminishes. The departures between the different results are smaller.

7. DISCUSSION OF RESULTS: INFLUENCE OF THE MAIN COLLISION INTEGRALS

In spite of the apparent satisfactory agreement between these calculated values and previous theoretical or experimental published works, the "accuracy" of results should be discussed. As previously mentioned, the transport coefficients depend on both population number densities and collision integrals. In air plasmas, as soon as the temperature reaches 10,000 K, the most numerous species are electrons, monatomic, positive ions, neutral atomic oxygen, and neutral atomic nitrogen. Collision integrals between these species play a particular role. Collision integrals between
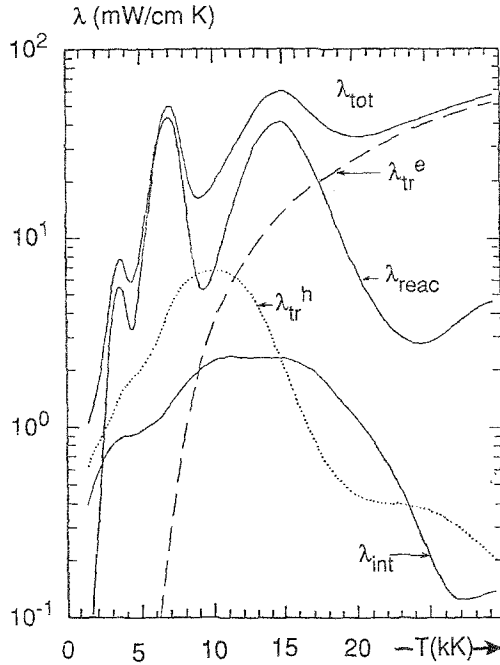
λ (mW/cm K)

Fig. 6. Components of the thermal conductivity for an air plasma at atmospheric pressure.

charged particles have been extensively discussed, and the model used in this work seems to be satisfactory whatever the value of the ionization degree.

The rigid-sphere model is particularly rough (but easy to use) to treat interaction between neutral particles. For the N–O interaction, the Morse potential associated with the ground electronic configuration of the NO molecule has been used alternatively. With respect to the collision integral calculated with the rigid-sphere model, $\Omega_{N-O}^{1,1}$ is then multiplied by a factor near 3. In Figs. 10 and 11, evolutions of the total thermal conductivity and the viscosity vs. temperature obtained with these two models are compared. For intermediate temperature values, i.e., between 7000 and 20,000 K, the increase of this particular collision integral leads to a decrease of λ_{tot} which can be as high as 35% for $p = 1$ atm. The reactive thermal conductivity λ_{reac} is strongly affected by this modification. The factor which represents the ratio between $\Omega_{NO}^{11\,Morse}$ and $\Omega_{NO}^{11\,R.S.}$ propagates up to a dividing factor 1.40 in λ_{reac}; λ_{tr}^h is also affected, but its weight in λ_{tot} is lower.

As the pressure grows, the maximum difference between the two evolutions is shifted toward the higher temperatures as the chemical equilibrium is displaced. Departures on the viscosity are greater: they can reach 60% near 10,000 K for $p = 1$ atm.
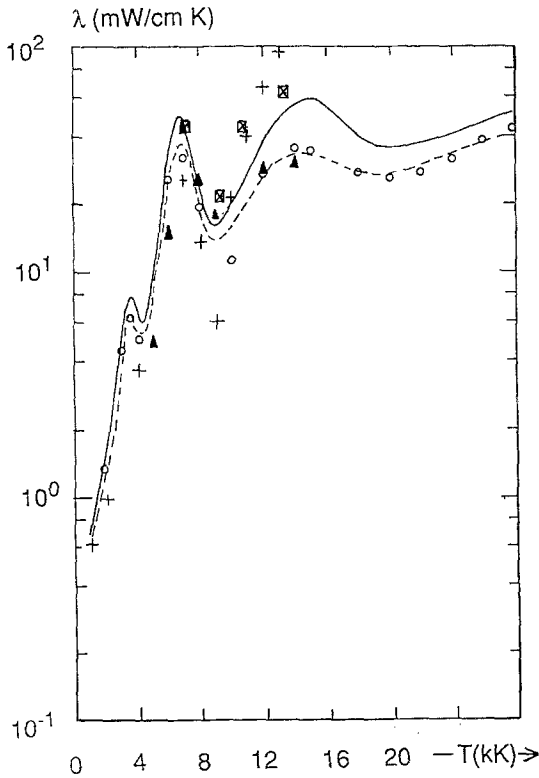
Fig. 7. Comparison of thermal conductivity values for a pressure of 1 atm: ○ (Ref. 40); + (Ref. 43); ▲ (Ref. 39); - - - (Ref. 42); —— (this work); □ (Ref. 47).

Values of the transport coefficients are not seriously affected when interaction between N and O^+ is treated on the basis of the Morse potential associated with the NO^+ molecular ion in its ground electronic configuration, because the polarizability model and Morse potential lead to relatively close values.

As shown by Capitelli,[48,46] collision integrals $\Omega^{1,1}$ for $N-N^+$ or $O-O^+$ interactions differ by as much as a factor of 2 according to the method used to compute the total charge-transfer cross section. For pure nitrogen or oxygen plasmas, the factor 2 plays a direct role on λ_{reac} and, due to the weight of this component, the incidence of these factors on λ_{tot} can reach 1.5. This maximum incidence is obtained for temperature values corresponding to the equilibria $|N| = |N^+|$ or $|O| = |O^+|$. In an air plasma at atmospheric pressure, these two equilibria are reached for temperatures of the same order of magnitude (14,700 and 15,500 K, respectively). When $\Omega^{1,1}_{NN^+}$ from
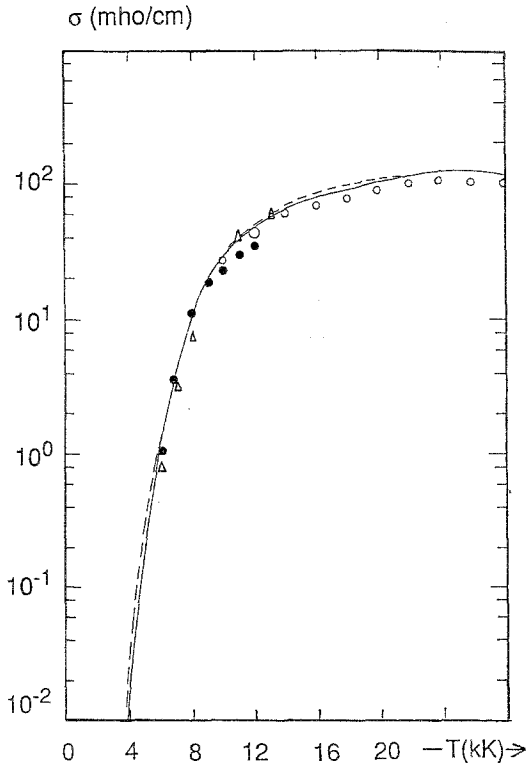
σ (mho/cm)

Fig. 8. Comparison of electrical conductivity values for a pressure of 1 atm: ○ (Ref. 40); ● (Ref. 44); ▲ (Ref. 39); - - - (Ref. 42); —— (this work).

Ref. 21 and $\Omega_{OO^+}^{1,1}$ from Ref. 23 are simultaneously multiplied by a factor 2, λ_{tot} can be divided by a factor whose maximum value (1.55) is obtained for a temperature slightly lower than 14,000 K at atmospheric pressure. As $\Omega_{NO}^{1,1}$, these two collision integrals play mainly on λ_{reac} and λ_{tr}^h and on the viscosity. In Figs. 12 and 13 the variation of λ_{tot} and η with temperature is shown.

Departures on transport parameter values induced by modification of the magnitude of these collision integrals should be considered as equivalent to error bars. This theoretical uncertainty is of the same order of magnitude as the experimental error bars obtained by some authors.

A detailed analysis of the influence on the reactive thermal conductivity of the charge exchange from the low-lying excited states (^4S, ^2D, ^2P for N atom, ^3P and ^1D for N$^+$ ion) can be found in Ref. 48 for a pure nitrogen plasma at atmospheric pressure.

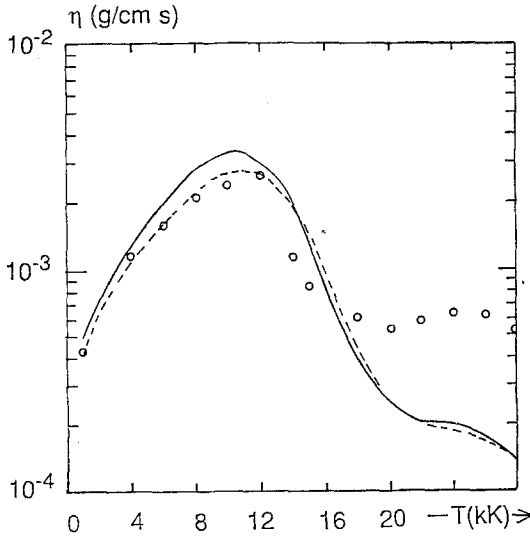**Fig. 9.** Comparison of viscosity values for a pressure of 1 atm: ○ (Ref. 40); – – – (Ref. 42); —— (this work).

When equilibrium situations are considered, the so-induced differences remain relatively weak (20% at maximum on λ_{reac} which propagates by 10% on λ_{tot}). In this work, the influence of the excited states is only considered through the component λ_{int}.

8. CONCLUSION

Numerical values of the transport coefficients of air plasmas, which are necessary, for instance, in solving the fundamental hydrodynamic equations governing plasma flow, have been obtained in extended ranges of pressure and temperature.

For pressures equal to or greater than 1 atm, air plasmas assumed in C.L.T.E. are characterized by a number of charged particles in the Debye sphere that is particularly low. Under these conditions, a difficulty arises when the formalism proposed by Liboff is used to treat interactions between charged particles: some high-order collision integrals have negative values, and this phenomenon is amplified when the pressure or the temperature increases. To avoid this difficulty, the model proposed by Mason, Munn, and Smith appears more appropriate: it can be used in the whole interval of pressure and temperature considered here, without giving rise to negative collision integral values.
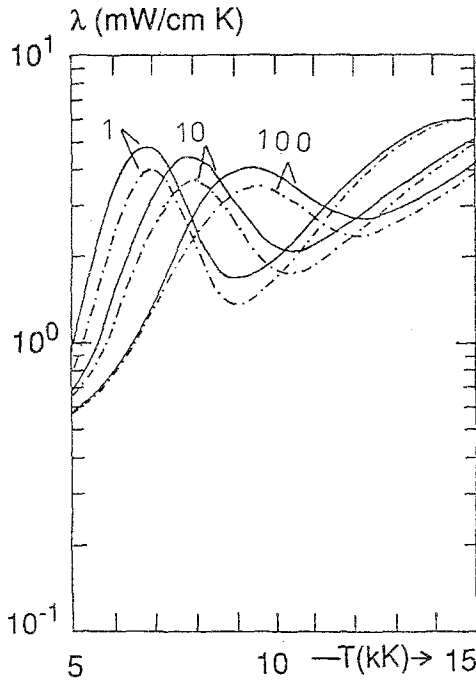
λ (mW/cm K)

Fig. 10. Influence of N–O interaction potential on the total thermal conductivity. ——— (rigid sphere); — · — (Morse potential).

η (g/cm s)

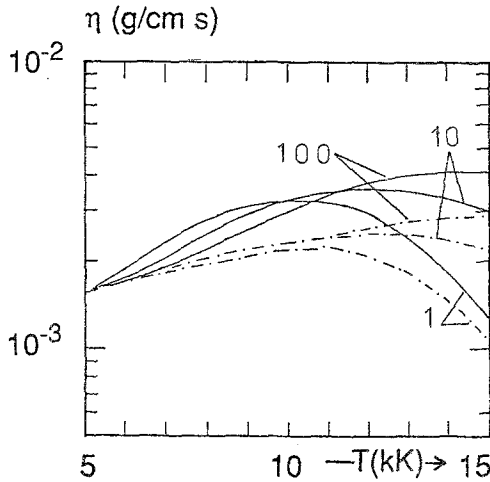**Fig. 11.** Influence of N–O interaction potential on the viscosity. ——— (rigid sphere); — · — (Morse potential).
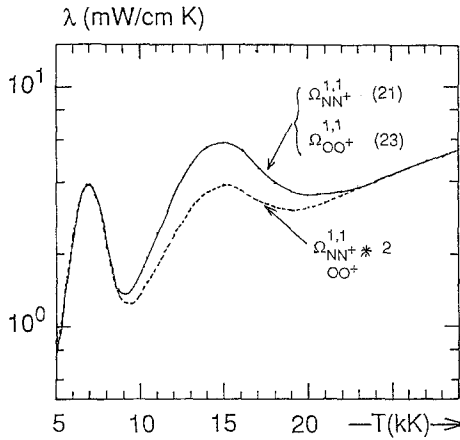
λ (mW/cm K)

Fig. 12. Influence of $\Omega^{1,1}_{NN^+}$ and $\Omega^{1,1}_{OO^+}$ on the total thermal conductivity for $P = 1$ atm.

The influence of the plasma composition on the transport coefficients can be illustrated by the following:

—For the lowest temperatures and the highest pressures considered in this work, the internal thermal conductivity represents up to 50% of the total thermal conductivity. This result contrasts with similar calculations performed for monatomic gases in which λ_{int} is generally negligible. This is related mainly to the significant concentrations of the polyatomic species corresponding to the nitrogen oxides and their ions.
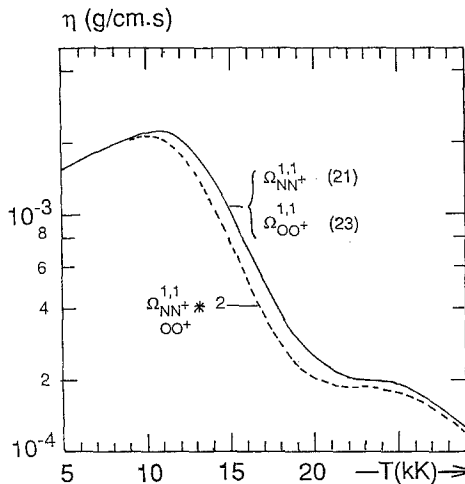
η (g/cm.s)

Fig. 13. Influence of $\Omega^{1,1}_{NN^+}$ and $\Omega^{1,1}_{OO^+}$ on the viscosity for $P = 1$ atm.

Introduction in the calculations of the nitrogen oxides also leads to a broadening of the peak of λ_{reac} near 3500 K and an increase of its area because in this range of temperatures the population number densities of these oxides show a maximum.

—For temperatures greater than 15,000 K, the influence of the multi-charged ions is particularly noticeable on the static viscosity value; this is in agreement with the analysis by Nicolet *et al.*

—Because at the lowest temperatures their concentration is not negligible with respect to the concentrations of electrons and positive ions, negative ions such as O^- and NO^- lead to a decrease in the electrical conductivity.

The influence of the choice of interaction potentials between particles has been examined at least for potentials between the major species of the plasma. This influence is noticeable for temperatures between 9000 and 20,000 K and give rise to an uncertainty up to 50% on total thermal conductivity and viscosity.

REFERENCES

1. J. Bacri and S. Raffanel, *Plasma Chem. Plasma. Process.* **7**, 53 (1987).
2. J. Bacri and S. Raffanel, Report No. 40277-86-2 (1986).
3. S. Chapman and T. G. Cowling, in *The Mathematical Theory of Non-uniform Gases,* Cambridge University Press, New York (1970).
4. J. O. Hirschfelder, C. F. Curtiss, and R. B. Bird, in *Molecular Theory of Gases and Liquids,* 2nd ed., Wiley, New York (1964), p. 464.
5. R. L. Liboff, *Phys. Fluids* **2**, 40 (1959).
6. T. Kihara, *J. Phys. Soc. Jpn.* **14**, 402 (1959).
7. R. S. Cohen, L. Spitzer, and P. R. McRoutly, *Phys. Rev.* **80**, 230 (1950).
8. L. Spitzer and R. Harm, *Phys. Rev.* **89**, 977 (1953).
9. F. J. Smith and R. J. Munn, *J. Chem. Phys.* **41**, 3560 (1964).
10. R. J. Munn, E. A. Mason, and F. J. Smith, *Phys. Fluids* **8**, 1103 (1965).
11. F. J. Smith, E. A. Mason, and R. J. Munn, *Phys. Fluids* **8**, 1907 (1965).
12. E. A. Mason, R. J. Munn, and F. J. Smith, *Phys. Fluids* **10**, 1827 (1967).
13. O. Aono, *Phys. Fluids* **11**, 341 (1968).
14. J. Glasser, Thesis Doct. es Sci., Université d'Orléans (1981).
15. R. S. Devoto, *Phys. Fluids* **16**, 616 (1973).
16. C. W. Allen, in *Astrophysical Quantities*, Athlone Press, London (1964).
17. E. V. Samoilov and N. N. Tsiterlauri, *High Temp.* **2**, 509 (1964).
18. E. V. Samoilov and N. N. Tsiterlauri, *High Temp.* **7**, 155 (1969).
19. F. J. Smith and R. J. Munn, *J. Chem. Phys.* **41**, 3560 (1964).
20. B. Rosen, in *Spectroscopic Data Relative to Diatomic Molecules*, Pergamon Press, Oxford (1970).
21. M. Capitelli and R. S. Devoto, *Phys. Fluids* **16**, 1835 (1973).
22. M. Eymard, 3rd Cycle Thesis No. 3101, Université de Toulouse (1984).
23. J. M. Mexmain, 3rd Cycle Thesis No. 83-81, Université de Limoges (1983).
24. J. Aubreton, Thesis Doct. es Sci., Université de Limoges (1985).

25. J. Aubreton, C. Bonnefoi, and J. M. Mexmain, *Rev. Phys. Appl.* **21**, 335, 1986.
26. T. Kihara, M. H. Taylor, and J. O. Hirschfelder, *Phys. Fluids* **3**, 5 (1960).
27. C. Nyeland and E. A. Mason, *Phys. Fluids* **10**, 985 (1967).
28. A. Dalgano and M. C. Maduel, *Proc. R. Soc. London* A **69**, 615 (1956); A. Dalgano, *Philos. Trans. R. Soc. London A* **250**, 426 (1958).
29. D. Rapp and W. E. Francis, *J. Chem. Phys.* **37**, 11 (1962).
30. N. Kobayashi, *J. Phys. Soc. Jpn.* **38**, 519 (1975).
31. N. G. Utterback and G. H. Miller, *Rev. Sci. Instrum.* **32**, 1101 (1961).
32. K. Penski, Proc. 4th Symp. Therm. Prop. (Amer. Soc. Mech. Eng.), College Park, New York (1968).
33. A. G. Engelhart, A. V. Phelps, and C. G. Risk, *Phys. Rev.* **135**, 1566 (1964).
34. R. S. Devoto, *Phys. Fluids* **9**, 1230 (1966).
35. R. S. Devoto, *Phys. Fluids* **10**, 2105 (1967).
36. K. S. Yun, S. Weissman, and E. A. Mason, *Phys. Fluids* **5**, 672 (1962).
37. J. N. Butler and R. S. Brokaw, *J. Chem. Phys.* **25**, 1636 (1957).
38. R. S. Brokaw and J. N. Butler, *J. Chem. Phys.* **32**, 1005 (1960).
39. E. I. Asinovski, A. V. Kirillin, E. P. Pakhomov, and V. I. Shabashov, *Proc. IEEE* **59**, 592 (1971).
40. J. M. Yos, Report AVCO RAD-TM-63-7, Wilmington, Massachusetts (1963).
42. T. C. Peng and A. L. Pindroh, 4th Biennial Gas Dyn. Symp. Amer. Rocket Soc., Evanston, Illinois, Paper No. 1995-61 (1961).
42. W. E. Nicolet, C. E. Shepard, K. J. Clark, A. Balakrishnan, J. P. Kesserling, K. E. Suchsland, and J. J. Reese, Jr., Report AEDC-TR-75-47 (1975).
43. C. F. Hansen, Report NASA TR-R-50, Ames Res. Center, Moffett Field (1959).
44. P. W. Schreiber, A. M. Hunter, and K. R. Benedetto, *AIAA J.* **11**, 815 (1973).
45. T. Chor-Weng, Ph.D. Thesis, University of Illinois (1963) pp. 54–55.
46. M. Capitelli, *J. Phys.* **38**, C3-227 (1977).
47. R. S. Devoto, U. H. Bauder, J. Cailleteau, and E. Shires, *Phys. Fluids* **21**, 552 (1978).
48. M. Capitelli, *J. Plasma Phys.* **14**, 365 (1975).